

# Detailed Photoluminescence Study of Doped and Co-Doped $\text{CeF}_3:\text{RE}^{3+}$ ( $\text{RE}^{3+} : \text{Nd}^{3+}, \text{Sm}^{3+}, \text{Eu}^{3+}, \text{Gd}^{3+}, \text{Tb}^{3+}, \text{Dy}^{3+}, \text{Ho}^{3+}, \text{Er}^{3+}, \text{Tm}^{3+}$ and $\text{Yb}^{3+}$ ) Nanophosphors with Energy Transfer Studies

Nayan Agrawal<sup>2,3</sup>, Harshita Bhatia<sup>2,4</sup>, Sakshi Anand<sup>2</sup>, Mayuri Gandhi<sup>1,3</sup>

Centre for Research in Nanotechnology & Research (CRNTS), Indian Institute of Technology, Powai, Mumbai, India  
Interns at IIT-B and Affiliated in Degree Programmes at Amity Institute of Nanotechnology, Amity University, Noida, Uttar Pradesh, India

Master Student at Biotechnology Centre, Technische Universität Dresden, Dresden, Germany

Intern at Karlsruhe Institute of Technology, Karlsruhe, Germany

**ABSTRACT:**  $\text{CeF}_3$  nanophosphors with remarkable optical properties have been proposed as possible phosphors for lighting and various bio-applications. In the present paper,  $\text{CeF}_3:\text{RE}^{3+}$  ( $\text{Ln}^{3+} : \text{Nd}^{3+}, \text{Sm}^{3+}, \text{Eu}^{3+}, \text{Gd}^{3+}, \text{Tb}^{3+}, \text{Dy}^{3+}, \text{Ho}^{3+}, \text{Er}^{3+}, \text{Tm}^{3+}$  and  $\text{Yb}^{3+}$ ) and  $\text{CeF}_3$  codoped ( $\text{Yb}^{3+}, \text{Nd}^{3+}$ ), ( $\text{Tb}^{3+}, \text{Yb}^{3+}$ ), ( $\text{Yb}^{3+}, \text{Eu}^{3+}$ ), ( $\text{Yb}^{3+}, \text{Ho}^{3+}$ ), ( $\text{Ho}^{3+}, \text{Nd}^{3+}$ ), ( $\text{Ho}^{3+}, \text{Er}^{3+}$ ), ( $\text{Yb}^{3+}, \text{Er}^{3+}$ ) ( $\text{Ho}^{3+}, \text{Tb}^{3+}$ ) nanocrystals were obtained by co-precipitation method. Nanoparticles of a spherical shaped morphology and particle size 9-12 nm were observed. X-Ray diffraction (XRD), high resolution-transmission electron microscopy (HR-TEM), Fourier transformed infrared spectroscopy (FT-IR), photoluminescence (PL) were employed to characterize the samples. A detailed energy level diagram that contains the position of the levels of all the trivalent lanthanide ions has been constructed for doped  $\text{CeF}_3$  and explained along with the energy transfer process from one dopant to the other in the codoped Cerium Fluoride nanophosphors. It has great potential applications in Light Emitting Devices, solid-state lasers, telecommunications, opto-electronics, biological labels and remote sensing.

**KEYWORDS:** Cerium Fluoride,  $\text{CeF}_3$ , Nanophosphor, Lanthanide, Rare earth, energy transfer, photoluminescence.

## I. INTRODUCTION

The Lanthanide ( $\text{Ln}^{3+}$ ) doped and co-doped luminescent fluoride nanomaterials are continuously gaining interest from scientific point of view [1-6]. The interest is largely credited to the intra 4-f transitions of the lanthanides that are quite sharp due to effective shielding of the 4f orbitals by the outer 5s and 5p orbitals. The absorption and emission properties of rare earth doped/Co-doped material can be further tailored by controlling the local environment, such as site symmetry, crystal field strength and electron phonon interaction strength of rare earth dopants.

Inorganic Fluorides Nanocrystal doped with Rare earth ions have shown unique luminescent properties & hence are a good candidate as host materials with corresponding useful application in optical telecommunication, laser, new optoelectronic devices & biological labels [7-13]. The fluoride lattice provides for the high co-ordination number for the Doped Rare earth ion and high ionicity of Rare earth and fluorine bond results in very wide Band gap, high density, high radiation resistance, fast response, low vibrational energies and low probability inter-configuration

# International Journal of Innovative Research in Science, Engineering and Technology

(An ISO 3297: 2007 Certified Organization)

Vol. 4, Issue 9, September 2015

transitions [14-16]. This results in long lifetime of their excited state & high luminescence quantum yields. Therefore, recently the investigation of doped and co-doped nano sized Rare earth fluorides has been increased manifolds [17-20]. Ce<sup>3+</sup> exhibits a very high UV absorption coefficient originated from allowed electric dipole 4f<sup>1</sup>5d transition. Taking Ce<sup>3+</sup> as a sensitizer, the efficient energy transfer from Ce<sup>3+</sup> to other Rare earth ion would result in strong RE emissions [21].

Rare earth when doped in some suitable host material displays the ability to convert lower wavelength photon into higher wavelength photon. This process of energy transfer is called Down-conversion. Initially, we had done doping of RE<sup>3+</sup> ions in the host matrix i.e. CeF<sub>3</sub> and further on co doping it was observed that the absorption and luminescence efficiency enhanced. Also, in the co-doping mechanism, one of the RE<sup>3+</sup> ions act as a sensitizer that absorbs the photon efficiently at certain wavelength and transfers the excitations to the other RE ion (acceptor ions). Transitional states of one element in the spectral region overlapped the spectral region of another element that resulted in the energy transfer from Ce<sup>3+</sup> to Ln<sup>3+</sup> and further resulted in intense peak. Hence, this is discussed in detail in the paper.

In the following study, CeF<sub>3</sub> was chosen as a base material and co-doping of RE<sup>3+</sup> ions (Nd<sup>3+</sup>, Sm<sup>3+</sup>, Eu<sup>3+</sup>, Gd<sup>3+</sup>, Tb<sup>3+</sup>, Dy<sup>3+</sup>, Ho<sup>3+</sup>, Er<sup>3+</sup>, Tm<sup>3+</sup> and Yb<sup>3+</sup>) into host matrix was done as it has low vibrational energies and therefore quenching of the excited state of the RE ions will be minimal. This is especially important for the RE<sup>3+</sup> ions emitting in the near IR part of the spectrum because they are sensitive to quenching by high-energy vibrations. Some of the RE<sup>3+</sup> ions like (Tb<sup>3+</sup>, Eu<sup>3+</sup>, Gd<sup>3+</sup>, Dy<sup>3+</sup> and Tm<sup>3+</sup>) emitted light in visible region i.e. from 490 nm to 690 nm whereas others like (Nd<sup>3+</sup>, Sm<sup>3+</sup>, Ho<sup>3+</sup>, Er<sup>3+</sup>, Yb<sup>3+</sup>) emitted light in IR region i.e. from 750 to 1550.

Various methods like physical, chemical & biological methods have been reported for the synthesis of nanophosphors with uniform size, morphology and composition. Here, we have used co-precipitation synthesis method to prepare the CeF<sub>3</sub> co-doped RE nanophosphors. In order to control the growth and agglomeration of the nanoparticles, organic surfactant, oleic acid was used. As controllable synthesis of lanthanide-doped nanoparticles has been done, it is observed that with rapidly shrinking size, the doped Nano-crystalline phosphor yields high luminescent efficiencies. Hence nano materials also display size and shape dependent properties.

## II. EXPERIMENTAL WORK

### **Reagents:**

All chemicals used are commercially available and were used as obtained, without further purification. The lanthanide salts Ce(NO<sub>3</sub>)<sub>3</sub>·6H<sub>2</sub>O, Nd(NO<sub>3</sub>)<sub>3</sub>·6H<sub>2</sub>O, Sm(NO<sub>3</sub>)<sub>3</sub>·6H<sub>2</sub>O, Eu(NO<sub>3</sub>)<sub>3</sub>·6H<sub>2</sub>O, Gd(NO<sub>3</sub>)<sub>3</sub>·6H<sub>2</sub>O, Tb(NO<sub>3</sub>)<sub>3</sub>·5H<sub>2</sub>O, Dy(NO<sub>3</sub>)<sub>3</sub>·6H<sub>2</sub>O, Ho(NO<sub>3</sub>)<sub>3</sub>·5H<sub>2</sub>O, Er(NO<sub>3</sub>)<sub>3</sub>·5H<sub>2</sub>O, Tm(NO<sub>3</sub>)<sub>3</sub>·6H<sub>2</sub>O, Yb(NO<sub>3</sub>)<sub>3</sub>·5H<sub>2</sub>O and Ammonium fluoride were used, all having a purity of 99.9 %. All the chemicals were purchased from Sigma-Aldrich and Oleic acid used was purchased from Merck.

### **Synthesis of lanthanum ion doped cerium fluoride nanoparticles; CeF<sub>3</sub>:RE<sup>3+</sup> (RE<sup>3+</sup> : Nd<sup>3+</sup>, Sm<sup>3+</sup>, Eu<sup>3+</sup>, Gd<sup>3+</sup>, Tb<sup>3+</sup>, Dy<sup>3+</sup>, Ho<sup>3+</sup>, Er<sup>3+</sup>, Tm<sup>3+</sup> and Yb<sup>3+</sup>):**

CeF<sub>3</sub>nanophosphors doped with various RE<sup>3+</sup> ion (RE<sup>3+</sup> : Nd<sup>3+</sup>, Sm<sup>3+</sup>, Eu<sup>3+</sup>, Gd<sup>3+</sup>, Tb<sup>3+</sup>, Dy<sup>3+</sup>, Ho<sup>3+</sup>, Er<sup>3+</sup>, Tm<sup>3+</sup> and Yb<sup>3+</sup>) were synthesized by co-precipitation route. In a typical synthesis 20 ml ethanol, in which total 0.02 M of Ce(NO<sub>3</sub>)<sub>3</sub>·6H<sub>2</sub>O and the corresponding Rare earth nitrate and oleic acid (0.002M) were dissolved. 0.06 M ammonium fluoride was dissolved in 80 ml distilled water and is heated up to 70°C. Both solutions were mixed and stirred for 10 minutes. The nanoparticles were precipitated out by adding ethanol and was washed several times by centrifuging and dried under ambient conditions.

### **Material characterization:**

X-ray powder diffraction (XRD) data were collected using Philips powder diffractometer PW3040/60 X'pert Pro with Cu K $\alpha$  radiation. The electron diffraction and micrographs were recorded using JEOL JEM-2100F high-resolution transmission electron microscope (HRTEM). Photoluminescence spectra were acquired using Perkin Elmer LS 55 model.

### III. RESULTS AND DISCUSSION

As-prepared the doped CeF<sub>3</sub> nanocrystals were characterized in detail by XRD, HR-TEM, PL spectroscopy and FTIR.

#### X-Ray Diffraction study:

The X-Ray Diffraction (XRD) contributes in the investigation of the phase structures of the nanoparticles. Figure 1 shows the XRD Pattern of co-doped nanophosphors and the standard data for CeF<sub>3</sub>. The results of XRD indicate that the samples synthesized are well crystallized, and the pattern is consistent with the hexagonal phase structure known from the bulk CeF<sub>3</sub> crystal (JCPDS: 08-0045).

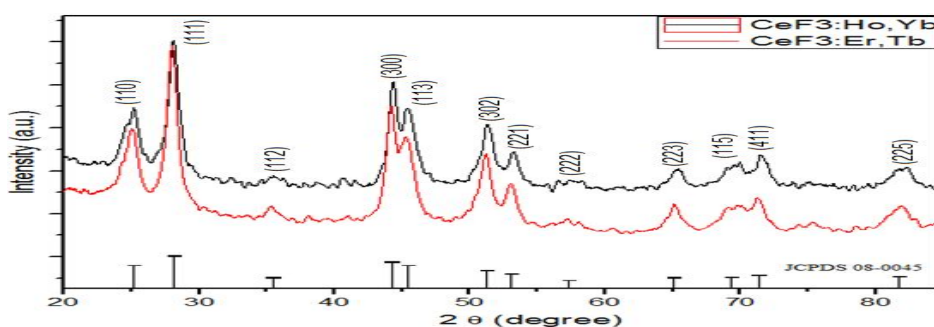


**Figure 1:** XRD spectra of CeF<sub>3</sub> co-doped with Ho, Yb and Er, Tb compared with the standard CeF<sub>3</sub> pattern.

Additionally, no other peak can be found in the patterns, revealing that there is no impurity in the products. Hence, it is exhibited that the parent structure was retained in the doubly doped samples.

In general, the nanocrystallite size can be estimated from the Debye-Scherrer equation as follows:

$$D = 0.941\lambda / (\beta \cos \theta)$$

Where D is the average grain size,  $\lambda$  is the x-ray wavelength (0.15405 nm), and  $\theta$  and  $\beta$  are the diffraction angle and Full Width at Half Maximum (FWHM) of an observed peak, respectively. The average crystallite sizes of CeF<sub>3</sub>: Eu, CeF<sub>3</sub>: Tb doped nanoparticles were determined as 18.292 nm and 12.803 nm respectively, by using the strongest peak (111) at  $2\theta = 28.17^\circ$ . Similarly, average crystalline sizes of the co-doped CeF<sub>3</sub>: Ho, Yb and Er, Tb nanophosphors were calculated to be in the range of 14-37 nm.

#### HR-TEM Studies:

The High Resolution TEM images for single and co-doped nanophosphors (figure.2 and figure.3 respectively) were recorded for particular compositions. TEM images of scales: 50 nm, 10 nm and 2 nm depict the particle size and shape of CeF<sub>3</sub>: Tb nanophosphor whereas scales: 50 nm, 10 nm, 5 nm, 2 nm depict the same CeF<sub>3</sub>: co-doped phosphor. The HR-TEM results show that the particles are spherical in shape and are crystalline in nature. In figure 2c and 3e (scale 2 nm) change in the surface morphology depicted that the dopant successfully got embedded into the lattices. The selected area electron diffraction (SAED) pattern indicated the diffraction to be polycrystalline in nature owing to the clusters of particles at different orientation otherwise each of them is single crystal. Figure 2d and 3b shows seven diffuse diffraction rings, which can be indexed as the (110), (111), (112), (300), (113), (302) and (221) phases of the hexagonal CeF<sub>3</sub> starting from the inner to the outer ring, which is in good agreement with the XRD patterns.

The energy-dispersive X-ray spectrum (EDS) of the sample CeF<sub>3</sub>: Tb (fig 2e) confirms the presence of small amount of Tb in CeF<sub>3</sub> nanophosphors.

## International Journal of Innovative Research in Science, Engineering and Technology

(An ISO 3297: 2007 Certified Organization)

Vol. 4, Issue 9, September 2015

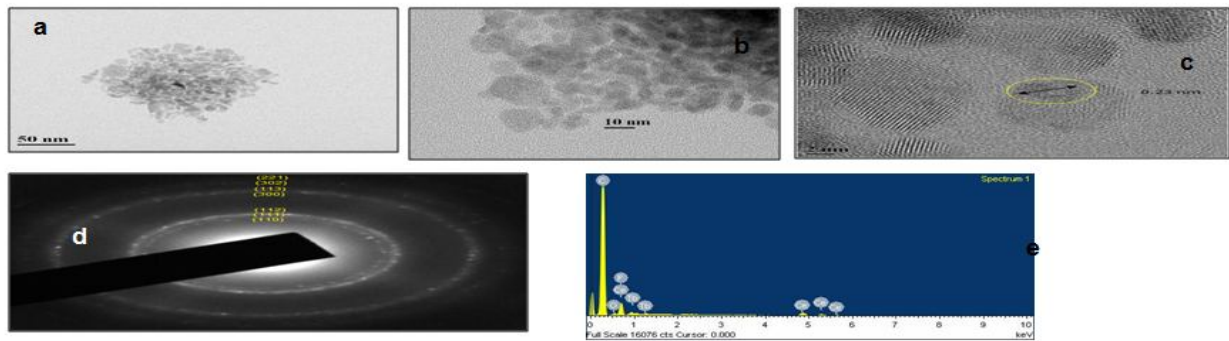


**Figure 2:** HR-TEM images of CeF3 singly doped at different scales along with SAED and EDS images. a) Scale 50 nm b) Scale 10 nm c) Scale 2 nm d) SAED e) EDS.

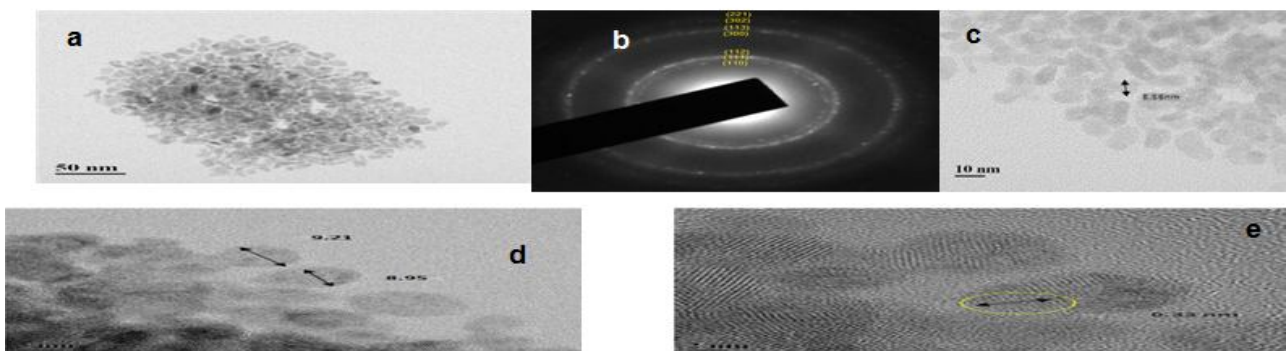


**Figure 3:** HR-TEM images of CeF3 co-doped at different scales along with SAED image. a) Scale 50nm b) SAED c) Scale 10nm d) Scale 5nm e) Scale 2nm.

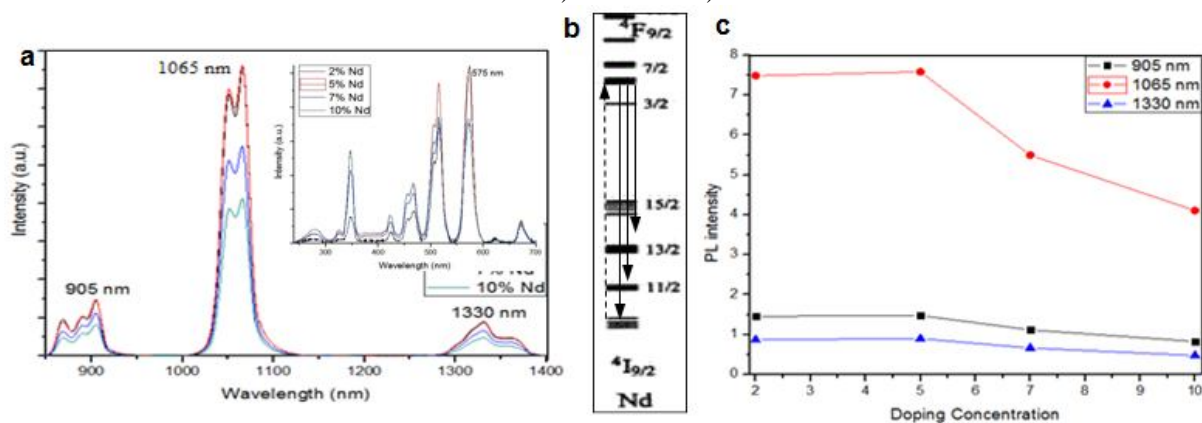


**Figure 4:** a) PL emission spectrum of CeF3:Nd3+ nanoparticles (x = 2, 5, 7, and 10 mol%) obtained after exciting the sample at 575 nm. Right inset shows the excitation spectrum;  $\lambda_{em} = 1065$  nm. b) Energy state diagram for Nd3+ c) PL intensity vs. Doping concentration graph for Nd3+.

## International Journal of Innovative Research in Science, Engineering and Technology

(An ISO 3297: 2007 Certified Organization)

Vol. 4, Issue 9, September 2015

Detailed PL studies were carried out on CeF<sub>3</sub> doped with varying concentrations of RE<sup>3+</sup> ions (RE<sup>3+</sup>: Nd, Sm, Eu, Gd, Tb, Dy, Ho, Er, Tm, Yb). The excitation and emission spectra of CeF<sub>3</sub>: x mol% RE<sup>3+</sup> samples (x= 2, 5, 7, 10) were taken.

The PL spectra of the CeF<sub>3</sub>: xNd<sup>3+</sup> (x = 2, 5, 7, 10 mol%) system showed a major excitation peak at 575nm (inset figure 4a). The corresponding emission spectra (figure 4a) were monitored from 800 nm to 1400 nm in which the peaks were observed at 905 nm, 1065 nm and 1330 nm that are assigned to 4F<sub>3/2</sub> → 4I<sub>γ</sub> (γ= 9/2, 11/2, 13/2) transitions respectively (figure 4b). Similar characteristic Nd<sup>3+</sup> emission profile was observed for all the composition. Maximum intensity was observed at 1065nm. Figure 4c illustrates the dependence of PL intensities of the three peaks upon the Nd<sup>3+</sup> doping concentrations of CeF<sub>3</sub> nanophosphors upon excitation at 575 nm. It is noticed that the PL intensity at 1065nm increases slightly as we move from 2 mol% to 5 mol% doping concentration, but decreases rapidly thereafter with the concentrations ranging from 5-10 mol %. Therefore the maximum emission intensity has been obtained upon optimizing the Nd<sup>3+</sup> concentration at 5%.

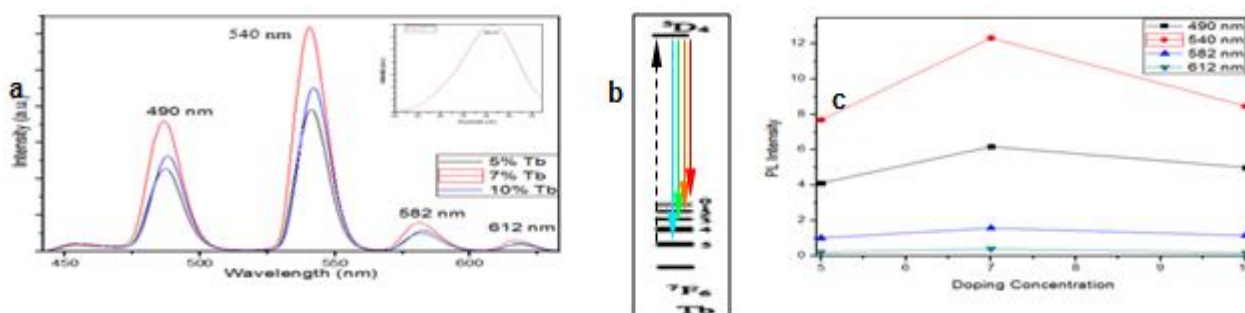


**Figure 5:** a) PL emission spectrum of CeF<sub>3</sub>:Tb<sup>3+</sup> nanoparticles (x = 5, 7, and 10 mol%) obtained after exciting the sample at 282 nm. Right inset shows the excitation spectrum;  $\lambda_{em} = 540$  nm. b) Energy state diagram for Tb<sup>3+</sup> c) PL intensity vs. Doping concentration graph for Tb<sup>3+</sup>.

The emission spectrum of the CeF<sub>3</sub>:xTb<sup>3+</sup> (x = 5,7,10 mol%) system, monitored from 440 nm to 640 nm, is dominated by intense green emissions at 490 nm, 540 nm, 582 nm and 612 nm, which are due to transitions from 5D<sub>4</sub> → 7F<sub>J</sub> (J=0, 1, 2, 3) energy states of Tb<sup>3+</sup> (fig 5a). The excitation spectrum corresponding to the main emission at 540 nm (5D<sub>4</sub> → 7F<sub>2</sub>) shows peak at 282 nm. (F-d transition of Tb<sup>3+</sup>) (Inset in Figure 5a). Fig. 5c gives the PL intensity vs. Tb<sup>3+</sup> doping concentrations of CeF<sub>3</sub> nanophosphors and the maximum intensity was observed when it was doped with 7 mol%.

In the case of Eu<sup>3+</sup> as the dopant, characteristic Eu<sup>3+</sup> emissions at 590 nm (5D<sub>0</sub> → 7F<sub>1</sub>), 612 nm (5D<sub>0</sub> → 7F<sub>2</sub>) and at 690 nm (5D<sub>0</sub> → 7F<sub>4</sub>) were observed (Figure 6a). The excitation spectrum corresponding to the main emission at 612 nm is characterized by the broad bands peaking at 280 nm and a sharp peak at 320 nm (which is the direct excitation for Eu<sup>3+</sup>). The PL intensity vs. doping concentration gave the maximum Eu<sup>3+</sup> doping concentration at 7 mol%. (Figure 6c)



## International Journal of Innovative Research in Science, Engineering and Technology

(An ISO 3297: 2007 Certified Organization)

Vol. 4, Issue 9, September 2015

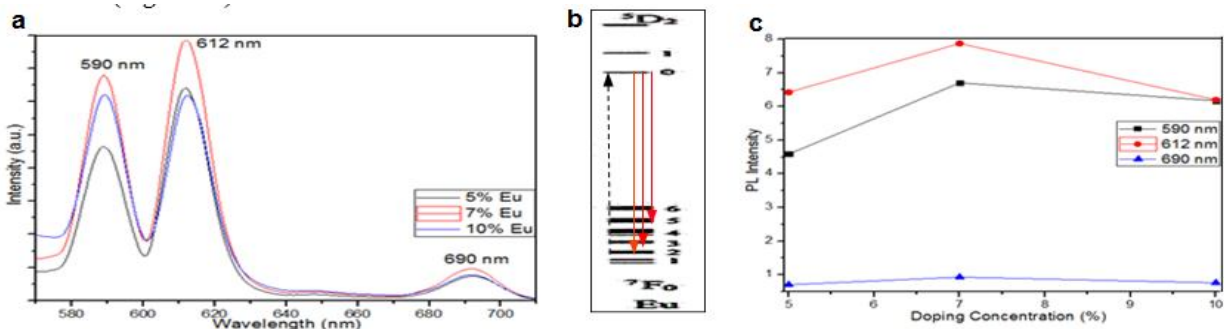


**Figure 6:** a) PL emission spectrum of CeF<sub>3</sub>:Eu<sup>3+</sup> nanoparticles (x = 2, 5, 7, and 10 mol %) obtained after exciting the sample at 320 nm. b) Energy state diagram for Eu<sup>3+</sup> c) PL intensity Vs Doping concentration graph for Eu<sup>3+</sup>.

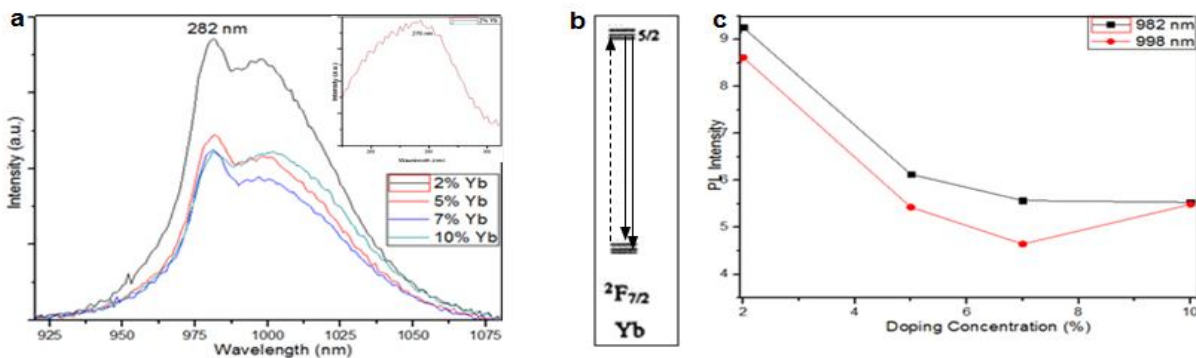


**Figure 7:** a) PL emission spectrum of CeF<sub>3</sub>:Yb<sup>3+</sup> nanoparticles (x = 2, 5, 7, and 10 mol %) obtained after exciting the sample at 282 nm. Right inset shows the excitation spectrum;  $\lambda_{em} = 982$  nm. b) Energy state diagram for Yb<sup>3+</sup> c) PL intensity Vs Doping concentration graph for Yb<sup>3+</sup>.

The CeF<sub>3</sub> : xYb<sup>3+</sup> (x = 2,5,7,10mol %) system when excited at 282 nm shows emission peaks at 982 nm (<sup>2</sup>E<sub>5/2</sub> → <sup>2</sup>F<sub>7/2</sub>) and 998 nm (<sup>2</sup>E<sub>5/2</sub> → <sup>2</sup>F<sub>9/2</sub>) which are the characteristics of Yb<sup>3+</sup> emission spectrum (figure 7a). Maximum intensity was observed at 982 nm. In this case the maximum PL intensity was observed in 2mol% Yb<sup>3+</sup> doped CeF<sub>3</sub> nanophosphors as shown in figure 7c.

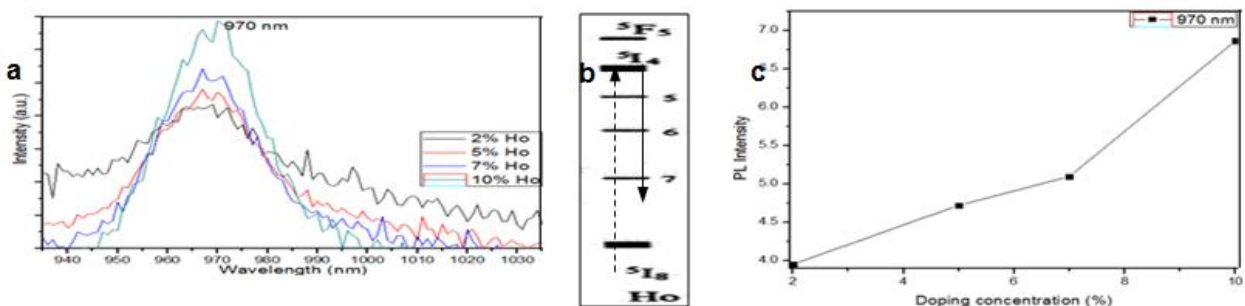


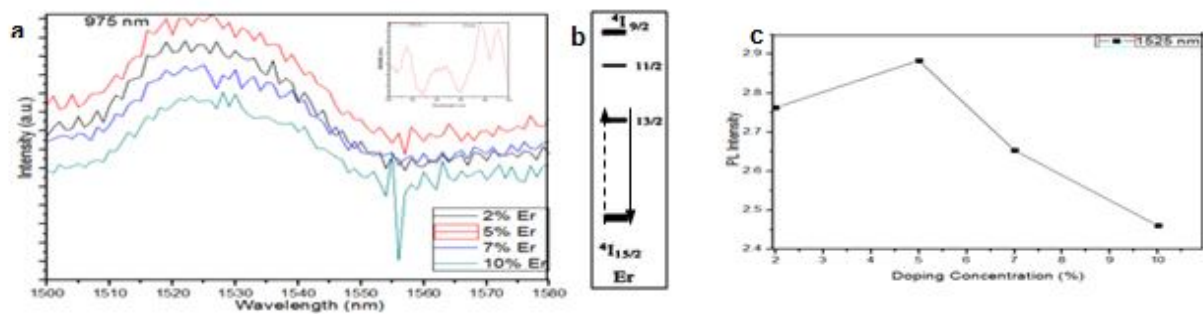
**Figure 8:** a) PL emission spectrum of CeF<sub>3</sub>:Ho<sup>3+</sup> nanoparticles (x = 2, 5, 7, and 10 mol %) obtained after exciting the sample at 445 nm. b) Energy state diagram for Ho<sup>3+</sup> c) PL intensity Vs Doping concentration graph for Ho<sup>3+</sup>.

## International Journal of Innovative Research in Science, Engineering and Technology

(An ISO 3297: 2007 Certified Organization)

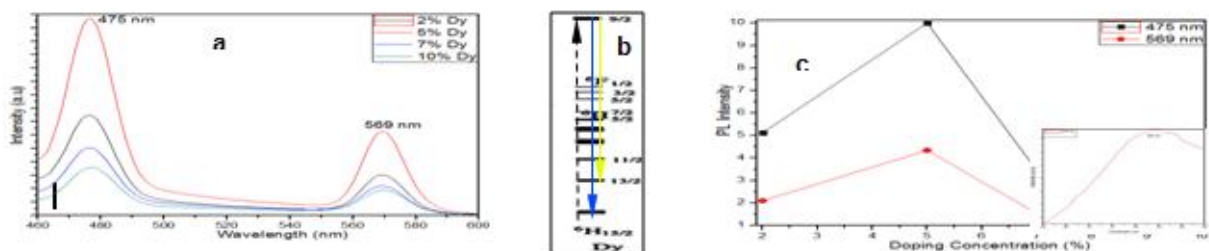
Vol. 4, Issue 9, September 2015

Figure 8a shows the emission spectrum of the CeF<sub>3</sub>:xHo<sup>3+</sup> (x = 2, 5, 7, and 10 mol %) system, obtained after exciting the sample at 445 nm. Intense peak was observed at 970 nm that corresponds to 5F<sub>5</sub> → 5I<sub>7</sub> Ho<sup>3+</sup> energy state transition. The maximum intensity was observed at 10mol% Ho<sup>3+</sup> concentration, figure 8c.



**Figure 9:** a) PL emission spectrum of CeF<sub>3</sub>:Er<sup>3+</sup> nanoparticles (x = 2, 5, 7, and 10 mol %) obtained after exciting the sample at 975 nm. b) Energy state diagram for Er<sup>3+</sup> c) PL intensity Vs Doping concentration graph for Er<sup>3+</sup>. Right inset shows the excitation spectrum;  $\lambda_{em} = 1525$  nm.

The excitation and emission spectra of the CeF<sub>3</sub>:xEr<sup>3+</sup> (x = 2, 5, 7, 10mol %) system is shown in fig 9a. The system after excitation at 975 nm showed the emission at 1525 nm, which was corresponding to 4I<sub>13/2</sub> → 4I<sub>15/2</sub> Er<sup>3+</sup> energy state transition (fig. 9b). PL intensity vs. doping concentration study in fig. 9c showed that intensity increases slightly as we move from 2mol% to 5mol% concentration, but decreases rapidly thereafter. Hence the maximum intensity is obtained at 5mol% Er<sup>3+</sup> doping concentration.



**Figure 10:** a) PL emission spectrum of CeF<sub>3</sub>:Dy<sup>3+</sup> nanoparticles (x = 2, 5, 7, and 10 mol %) obtained after exciting the sample at 282 nm. b) Energy state diagram for Dy<sup>3+</sup> c) PL intensity Vs Doping concentration graph for Dy<sup>3+</sup>. Right inset shows the excitation spectrum;  $\lambda_{em} = 475$  nm

The CeF<sub>3</sub>:xDy<sup>3+</sup> (x = 2, 5, 7, 10mol%) system showed emission peaks at 475 nm (4F<sub>9/2</sub> → 6H<sub>15/2</sub>) and 569 nm (4F<sub>9/2</sub> → 6H<sub>13/2</sub>) after it was excited at 282nm as displayed in Fig.10a and in the inset of Fig. 10c. The peak at 475 nm was most intense, giving the system the characteristic blue-green color. The optimum doping concentration was observed to be at 5mol% for Dysprosium (Figure 10c).

## International Journal of Innovative Research in Science, Engineering and Technology

(An ISO 3297: 2007 Certified Organization)

Vol. 4, Issue 9, September 2015

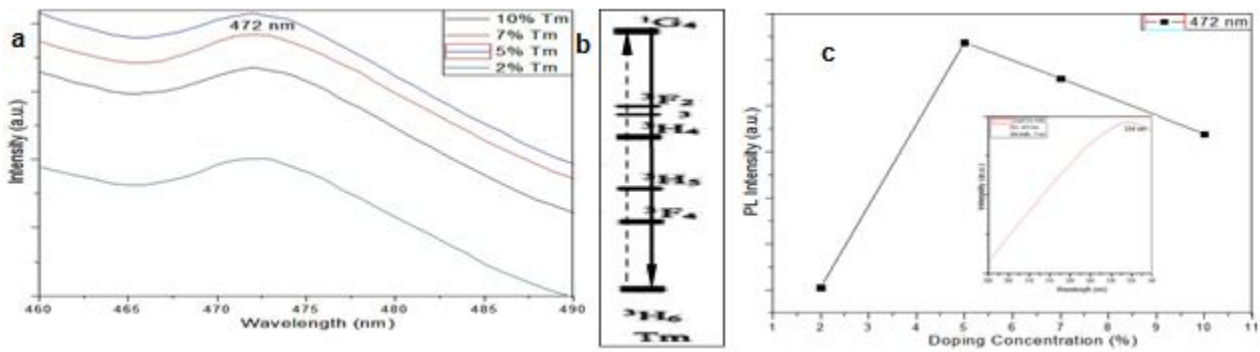


**Figure 11:** a) PL emission spectrum of CeF<sub>3</sub>:Tm<sup>3+</sup> nanoparticles (x = 2, 5, 7, and 10 mol%) obtained after exciting the sample at 334 nm. b) Energy state diagram for Tm<sup>3+</sup> c) PL intensity vs. Doping concentration graph for Tm<sup>3+</sup>. Right inset shows the excitation spectrum;  $\lambda_{em} = 472$  nm.

The excitation and emission spectra of the CeF<sub>3</sub>: xTm<sup>3+</sup> (x = 2, 5, 7, 10 mol%) system is shown in figure 11a. The system after excitation at 334 nm showed the emission at 472 nm, which was corresponding to 1G<sub>4</sub> → 3G<sub>6</sub> Tm<sup>3+</sup> energy state transition (fig 11b). PL intensity vs. doping concentration study showed that intensity increases as we move from 2 mol% to 5 mol% concentration (fig 11c), but decreases slightly thereafter. Hence the maximum PL intensity is obtained at 5 mol% Tm<sup>3+</sup> doping concentration.

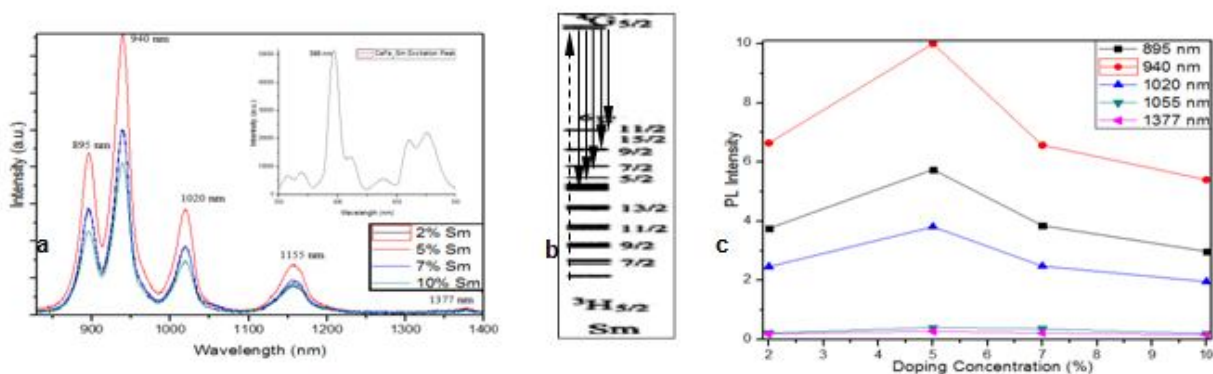


**Figure 12:** a) PL emission spectrum of CeF<sub>3</sub>:Sm<sup>3+</sup> nanoparticles (x = 2, 5, 7, and 10 mol %) obtained after exciting the sample at 398 nm. Right inset shows the excitation spectrum;  $\lambda_{em} = 940$  nm. b) Energy state diagram for Sm<sup>3+</sup> c) PL intensity vs. Doping concentration graph for Sm<sup>3+</sup>.

The Excitation spectra of the CeF<sub>3</sub>: xSm<sup>3+</sup> (x = 2, 5, 7, 10 mol%) system showed intense peak at 398 nm (inset fig 12a). The corresponding emission spectrum was monitored in the IR Region from 800 nm to 1400 nm. Multiple peaks were observed at 895 nm, 940 nm, 1020 nm, 1155 nm and 1377 nm that are assigned to 4G<sub>5/2</sub> → 6F<sub>y</sub> (y = 3/2 to 11/2) transitions respectively (figure 12b). Similar characteristic Sm<sup>3+</sup> emission profile was observed for all the composition. Maximum PL intensity was observed at 940 nm. Figure 12c illustrates the dependence of PL intensity upon the Sm<sup>3+</sup> doping concentrations of CeF<sub>3</sub> nanophosphors upon excitation at 398 nm. It is noticed that the PL intensity increases as we move from 2 mol% to 5 mol% doping concentration, but decreases rapidly thereafter with the concentrations ranging from 5-10 mol%. Therefore the maximum emission has been obtained upon optimizing the Sm<sup>3+</sup> concentration at 5 mol%.



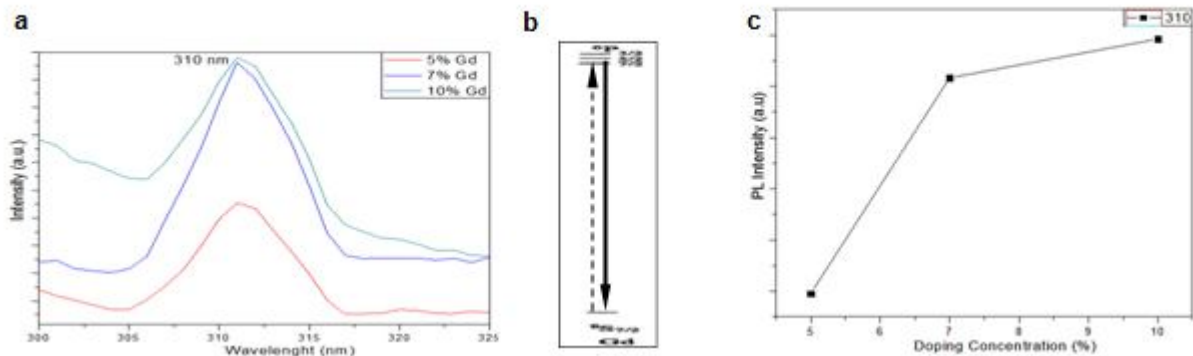


**Figure 13:** a) PL emission spectrum of CeF<sub>3</sub>: Gd<sup>3+</sup> nanoparticles (x = 2, 5, 7, and 10 mol%) obtained after exciting the sample at 274 nm. b) Energy state diagram for Gd<sup>3+</sup> c) PL intensity vs. Doping concentration graph for Gd<sup>3+</sup>.

The emission spectrum (figure. 13a) of the CeF<sub>3</sub>x:Gd<sup>3+</sup> (x = 2,5,7,10 mol%) system, monitored from 300 nm to 325 nm, is dominated by intense emission at 310 nm, which is due to transitions from <sup>6</sup>P<sub>7/2</sub> → <sup>8</sup>S<sub>7/2</sub> energy states of Gd<sup>3+</sup> (figure 13b) when excited at 274 nm. Figure 13c gives the PL intensity vs. Gd<sup>3+</sup> doping concentrations of CeF<sub>3</sub> Nanophosphors and the maximum intensity was observed when it was doped with 7 mol%.

**Photoluminescence (PL) Studies of co-doped nanophosphor of CeF<sub>3</sub>:**

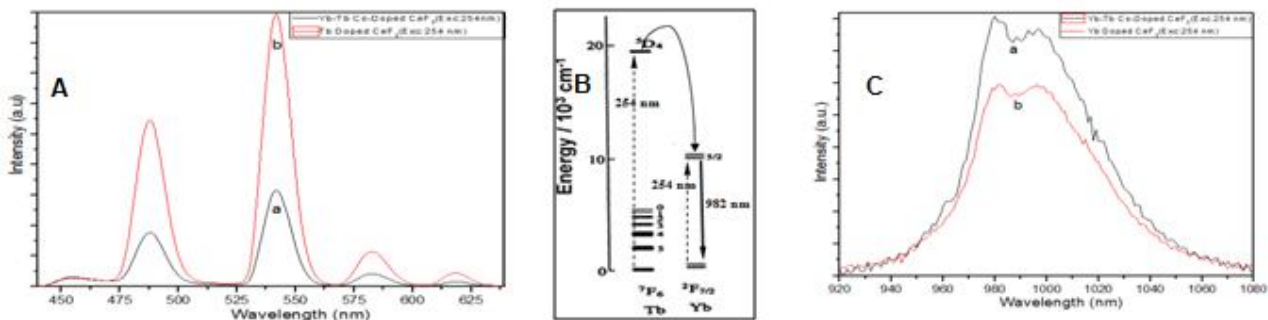


**Figure 14:** A) PL emission of CeF<sub>3</sub>:Yb, Tb and CeF<sub>3</sub>:Tb obtained after exciting the sample at 254 nm. B) Energy state diagram for Tb<sup>3+</sup> and Yb<sup>3+</sup> and the corresponding energy transfer between the two. C) PL emission of CeF<sub>3</sub>:Yb, Tb and CeF<sub>3</sub>:Yb obtained after exciting the sample at 254 nm.

Detailed PL studies were carried out on CeF<sub>3</sub> co-doped with various RE<sup>3+</sup> ions (RE<sup>3+</sup> = Nd, Eu, Tb, Ho, Er, Yb). The emission spectra and detailed explanation of the energy transfer between the energy levels of the dopant was done with the depiction of simplified energy state diagram.

The PL spectra of CeF<sub>3</sub> doubly doped with Yb<sup>3+</sup>, Tb<sup>3+</sup> brought in interesting results (Fig 14A). It was previously observed in single doped CeF<sub>3</sub> studies that Tb<sup>3+</sup> and Yb<sup>3+</sup> when excited with 254 nm and 282 nm respectively gave their characteristic emissions, but when co-doped, Yb<sup>3+</sup> under the influence of Tb<sup>3+</sup> as a sensitizer showed better emission intensity at 254 nm.

## International Journal of Innovative Research in Science, Engineering and Technology

(An ISO 3297: 2007 Certified Organization)

Vol. 4, Issue 9, September 2015

A simple energy state diagram shows the mechanism behind the enhancement of Yb<sup>3+</sup> emission at 254 nm. (Fig 14B) Tb<sup>3+</sup> act as a sensitizer and absorbs the UV light first and then transfers the energy to Yb<sup>3+</sup> (acceptor) in the time scale of Pico-seconds or faster, which then radiates energy in the IR region. It was also observed that Tb<sup>3+</sup> emissions in the co-doped system were less intense, confirming that electrons from Tb<sup>3+</sup> get transferred to Yb<sup>3+</sup> and hence proving that Tb<sup>3+</sup> here acts as a sensitizer and Yb<sup>3+</sup> as an acceptor. T5

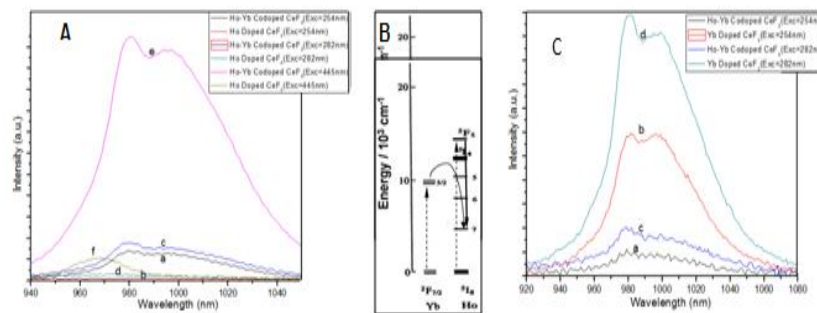


**Figure 15:** A) PL emission of CeF<sub>3</sub>:Ho, Yb and CeF<sub>3</sub>:Ho obtained after exciting the sample at 254 nm, 282 nm and 445 nm. B) Energy state diagram for Ho<sup>3+</sup> and Yb<sup>3+</sup> and the corresponding energy transfer between the two. C) PL emission of CeF<sub>3</sub>:Ho, Yb and CeF<sub>3</sub>:Yb obtained after exciting the sample at 254 nm and 285 nm.

The PL spectra (Fig 15A) of the CeF<sub>3</sub>: Ho, Yb system showed that Yb<sup>3+</sup> acts as a sensitizer which absorbs the energy and passes on to Ho<sup>3+</sup> (acceptor), hence giving better emission intensity. Ho<sup>3+</sup> gave better results at 254 nm, 282 nm as well as at 445 nm, corresponding to these excitation values; Yb<sup>3+</sup> gave a low emission intensity, indicating that Yb<sup>3+</sup> loses its energy to the acceptor (Figure 15C). The interaction between Yb<sup>3+</sup> and Ho<sup>3+</sup> was strong as intensity of all the Ho<sup>3+</sup> emissions increased significantly especially the one at 445 nm, which is a characteristic emission for Ho<sup>3+</sup>. The mechanism is depicted in figure 15B.

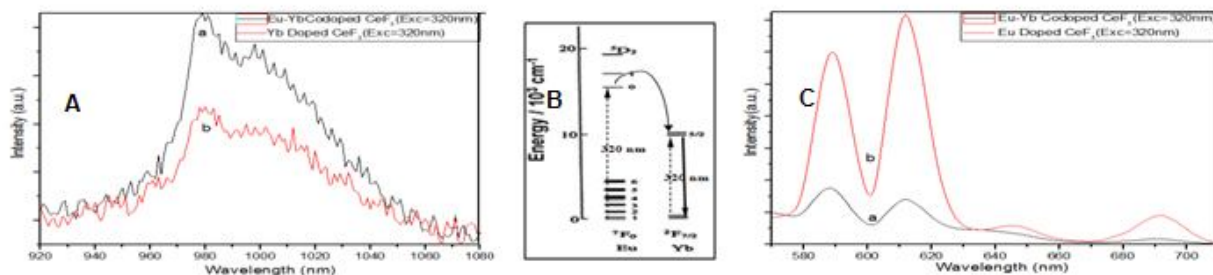


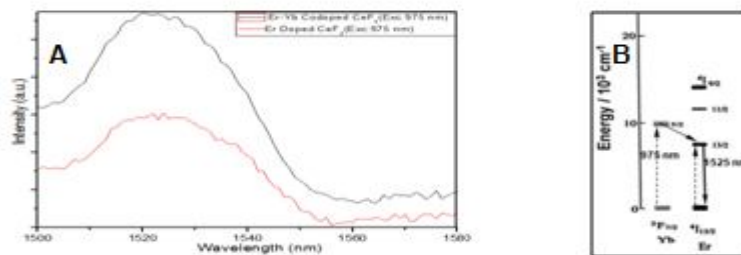
**Figure 16:** A) PL emission of CeF<sub>3</sub>: Eu, Yb and CeF<sub>3</sub>: Yb obtained after exciting the sample at 320 nm. B) Energy state diagram for Eu<sup>3+</sup> and Yb<sup>3+</sup> and the corresponding energy transfer between the two. C) PL emission of CeF<sub>3</sub>: Eu, Yb and CeF<sub>3</sub>: Eu obtained after exciting the sample at 320 nm

In the case of CeF<sub>3</sub>:Eu, Yb, Eu<sup>3+</sup> is the sensitizer which first accepts light when excited with 320 nm and then transfers it to Yb<sup>3+</sup> (acceptor). Significant increment in intensity was observed in this process and this suggested that the interaction between Yb<sup>3+</sup> and Eu<sup>3+</sup> was strong. The energy state diagram shows the process in simplified version. (Figure 16B)

## International Journal of Innovative Research in Science, Engineering and Technology

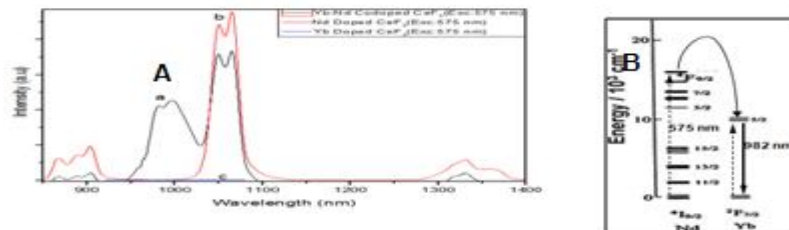
(An ISO 3297: 2007 Certified Organization)

Vol. 4, Issue 9, September 2015



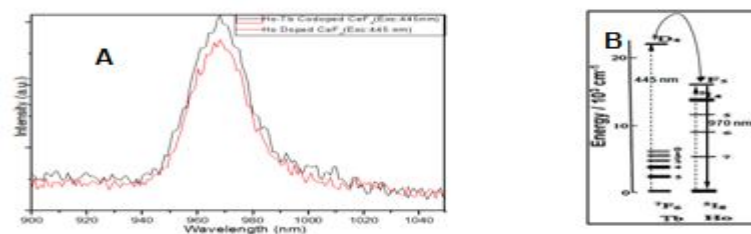
**Figure 17:** A) PL emission of CeF<sub>3</sub>: Er, Yb and CeF<sub>3</sub>: Er obtained after exciting the sample at 975 nm. B) Energy state diagram for Er<sup>3+</sup> and Yb<sup>3+</sup> and the corresponding energy transfer between the two.

In the CeF<sub>3</sub>:Er,Yb system the PL spectra (Fig 17A) shows that Yb<sup>3+</sup> successfully transfers light to Er<sup>3+</sup>, thus increasing the luminescence intensity significantly at 1525 nm, which is the characteristic emission for Er<sup>3+</sup>.



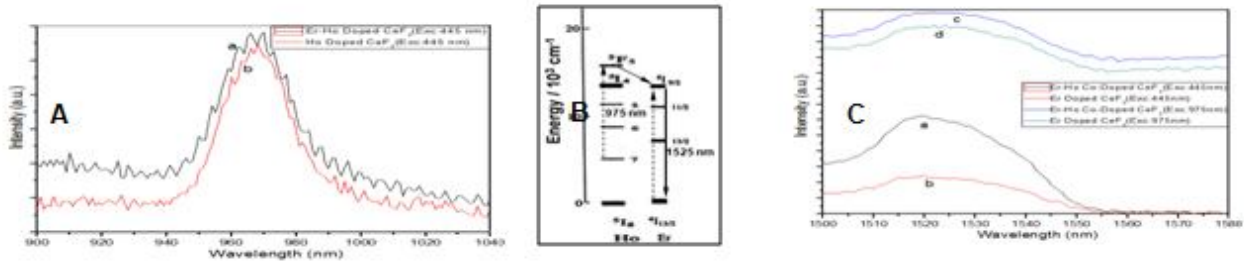
**Figure 18:** A) PL emission of CeF<sub>3</sub>: Nd, Yb, CeF<sub>3</sub>: Yb and CeF<sub>3</sub>: Nd obtained after exciting the sample at 575 nm. B) Energy state diagram for Nd<sup>3+</sup> and Yb<sup>3+</sup> and the corresponding energy transfer between the two.

Figure 18 shows the CeF<sub>3</sub>:Nd,Yb; Nd<sup>3+</sup> acts as a sensitizer for Yb<sup>3+</sup>, helping in the significantly large increment in the characteristics emission (982 nm) of Yb<sup>3+</sup> when excited with 575 nm. It was observed that when CeF<sub>3</sub> single doped Yb<sup>3+</sup> was excited at 575 nm, no peaks were obtained in the range 900 nm to 1080 nm, but in the presence of Nd<sup>3+</sup> as a Co-dopant, we get a large peak at 982 nm at the same excitation value. This is due to the transfer of energy from Nd<sup>3+</sup> to Yb<sup>3+</sup>.



**Figure 19:** A) PL emission of CeF<sub>3</sub>: Ho, Tb and CeF<sub>3</sub>: Ho obtained after exciting the sample at 445 nm. B) Energy state diagram for Ho<sup>3+</sup> and Tb<sup>3+</sup> and the corresponding energy transfer between the two.

The Ho<sup>3+</sup> and Tb<sup>3+</sup> interaction was considered (figure 019A). PL studies showed that Ho<sup>3+</sup> in the presence of Tb<sup>3+</sup> as a co-dopant gave a high intense peak at 970 nm, which intense compared to single doped Ho<sup>3+</sup>. Hence Tb<sup>3+</sup> here is the sensitizer and Ho<sup>3+</sup> the acceptor.



**Figure 20:** A) PL emission of CeF<sub>3</sub>: Er, Ho and CeF<sub>3</sub>: Ho obtained after exciting the sample at 445 nm. B) Energy state diagram for Er<sup>3+</sup> and Ho<sup>3+</sup> and the corresponding energy transfer between the two. C) PL emission of CeF<sub>3</sub>: Er, Ho and CeF<sub>3</sub>: Er obtained after exciting the sample at 445 nm and 975 nm.

In CeF<sub>3</sub>: Ho,Er, the PL spectra (fig 20A) showed that when excited with 445 nm and 975 nm, the co-doped system showed improved PL intensity on both the regions i.e. 900-1040 nm and 1500-1580 nm. Therefore, in this system both the dopants are complementing each other in terms of energy transfer.

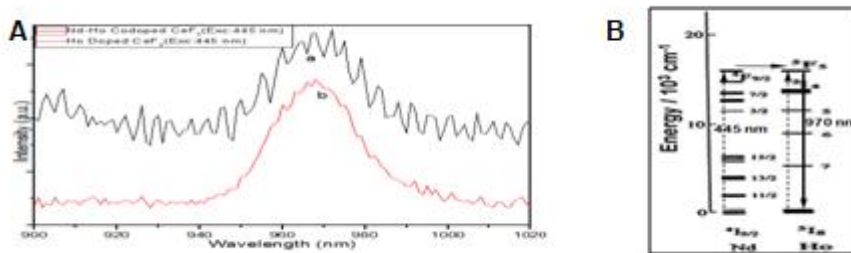


**Figure 21:** A) PL emission of CeF<sub>3</sub>: Nd, Ho and CeF<sub>3</sub>: Ho obtained after exciting the sample at 445 nm. B) Energy state diagram for Nd<sup>3+</sup> and Ho<sup>3+</sup> and the corresponding energy transfer between the two.

In CeF<sub>3</sub>:Ho<sup>3+</sup>, Nd<sup>3+</sup>, Nd transfers energy to Ho, and when excited with 445 nm (fig 21A), there is an increase in the PL intensity of the doped system. Hence Nd, acting as a sensitizer and Ho acts as an activator.

From above studies one can engineer a desired wavelength and it is summarized in Table 1 for doped and Table 2 for co-doped system in CeF<sub>3</sub>

**Table 1:** Doped CeF<sub>3</sub> with Excitation & emission wavelength and optimum concentration

No.	Ln <sup>3+</sup>	$\lambda_{em}$	$\lambda_{ex}$	Emission color	Optimum Concentration in mol%
1	Nd	575	1065	NIR	5
2	Tb	282	540	Green	7
3	Eu	320	610	Red	7
4	Yb	282	982	NIR	2
5	Ho	445	970	NIR	10
6	Er	975	1525	NIR	5
7	Dy	282	475	blue	2
8	Tm	334	472	blue	5
9	Sm	398	940	NIR	2
10	Gd	274	310	UV	10

## International Journal of Innovative Research in Science, Engineering and Technology

(An ISO 3297: 2007 Certified Organization)

Vol. 4, Issue 9, September 2015

**Table:2:** Co-doped CeF<sub>3</sub> with Excitation & emission wavelength and Energy Transfer

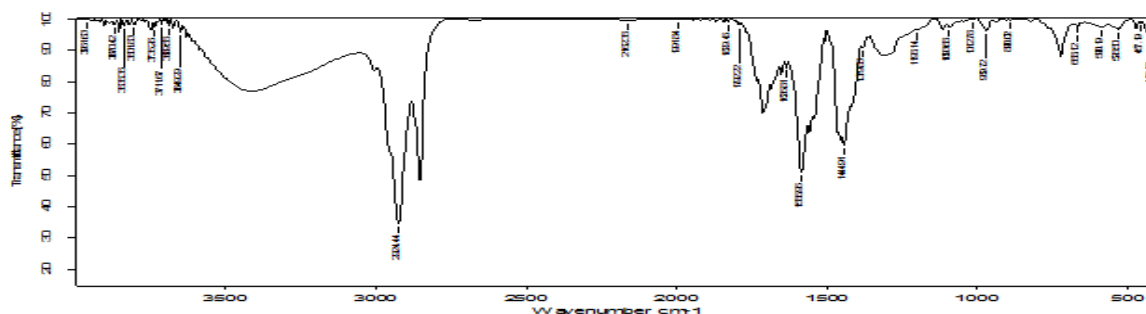
No.	Ln <sup>3+</sup> Co-doped	$\lambda_{ex}$	$\lambda_{em}$ range	Energy Transfer
1	Tb-Yb	254/282	400-700	Tb to Yb
2	Ho-Yb	282/445	940-1050	Yb to Ho
3	Eu-Yb	320	920-1080	Eu to Yb
4	Er-Yb	975	1500-1580	Yb to Er
5	Nd-Yb	575	800-1400	Nd to Yb
6	Ho-Tb	445	900- 1050	Tb to Ho
7	Ho-Er	445/975	900-1050	Ho to Er
8	Ho-Nd	445	900-1020	Nd to Ho

No.	Ln <sup>3+</sup> Co-doped	$\lambda_{ex}$	$\lambda_{em}$ range	Energy Transfer
1	Tb-Yb	254/282	400-700 920-1080	Tb to Yb
2	Ho-Yb	282/445	940-1050 920-1080	Yb to Ho
3	Eu-Yb	320	920-1080	Eu to Yb
4	Er-Yb	975	1500-1580	Yb to Er
5	Nd-Yb	575	800-1400	Nd to Yb
6	Ho-Tb	445	900- 1050	Tb to Ho
7	Ho-Er	445/975	900-1050 1500-1580	Ho to Er
8	Ho-Nd	445	900-1020	Nd to Ho

**FTIR studies:**

Fig. 22 shows the typical Fourier transform infrared (FT-IR) spectra of OA-modified CeF<sub>3</sub> doped with RE<sup>3+</sup>. Sample exhibits a strong absorption at 2852.31 and 2924.44 cm<sup>-1</sup> in the C–H stretching region (4000–1300 cm<sup>-1</sup>) attributable to the symmetric and asymmetric C–H stretches, respectively. The weak absorption at 2956.7 cm<sup>-1</sup> results from the asymmetric stretching of the terminal –CH<sub>3</sub> group of the alkyl chain. The peak at 3005.5 cm<sup>-1</sup> indicates that the C–H stretching is involved. Meanwhile, in the fingerprint region (below 1300 cm<sup>-1</sup>), the absorption at 721 cm<sup>-1</sup> clearly proves the existence of the (CH<sub>2</sub>)<sub>n</sub> (n >4) alkyl chains. A strong absorption was observed at 1712 cm<sup>-1</sup>, which is attributed to the stretching vibrations of the CO group. But, two characteristic bands centered at 1444 and 1585 cm<sup>-1</sup> were observed, which can be associated with the -COO<sup>2-</sup> asymmetric and symmetric stretching vibrations of carboxylate anions bound to the CeF<sub>3</sub> surface. Thus this proves the presence of Oleic acid in the sample. [22]



**Figure 22:** FTIR-spectra of CeF<sub>3</sub>



# International Journal of Innovative Research in Science, Engineering and Technology

(An ISO 3297: 2007 Certified Organization)

Vol. 4, Issue 9, September 2015

## IV.CONCLUSION

From the above studies, it has been observed that one can engineer the wavelength of emission or excitation by changing dopants or co-doping with RE<sup>3+</sup>. Many RE<sup>3+</sup> energy levels are of the same energy and can transfer their energy and intensify the peak of one to act as a sensitizer or activator. It has great potential applications in Light Emitting Devices, solid-state lasers, biological labels, remote sensing and opto-electronics.

## ACKNOWLEDGEMENTS

We would like to acknowledge DRDO for PL studies in this project. We are also thankful for the support and provision of instrument facilities by SAIF, IIT Bombay.

## REFERENCES

1. R. Gill, M. Zayats, I. Willner "Semiconductor Quantum Dots for bioanalysis", *Angewandte Chemie International Edition*, vol. 47, no.40, pp. 7602-7625.
2. L. Y. Wang, R. X. Yan, Z. Hao, L. Wang, J. H. Zeng, H. Bao, X. Wang, Q. Peng, Y. D. Li, "Fluorescence resonant energy transfer biosensor based on upconversion-luminescent nanoparticles *Angewandte Chemie International Edition*, vol.44, no.37, pp.6054-6057.
3. M. Wang, C. C. Mi, W. X. Wang, C. H. Liu, Y. F. Wu, Z. R. Xu, C. B. Mao, S. K. Xu, "Immunolabeling and NIR-Excited Fluorescent Imaging of HeLa Cells by Using NaYF<sub>4</sub>:Yb,Er Upconversion Nanoparticles," *American Chemical Society Nano*, vol.3, no.6, pp.1580-1586, May.20.
4. L. H. Slooff, A. Blaaderen, A. Polman, G. A. Hebbink, S. I. Klink, F. C. J. M. van Veggel, D. N. Reinhoudt, J. W. Hofstra, "Rare-earth doped polymers for planar optical amplifiers," *Journal of Applied Physics*, vol.91, no.7, pp.3955-3980, Apr.1.
5. A. Jha, "A review of visible, near-IR and mid-IR transitions in rare-earth doped glass waveguides for remote sensing and LIDAR," *Proc. SPIE*, 6409.
6. A. Ikesue, Y. L. Aung, T. Taira, T. Kamimura, K. Yoshida, G. L. Messing, "Progress in ceramic lasers," *Annual Review of Material Research*, vol.36, no.1, pp.397-429, Apr.10.
7. R. Bhargava, D. Gallagher, X. Hong, A. Nurmikko, "Optical Properties of Manganese-Doped Nanocrystals of ZnS," *Physical Review Letters*, vol.72, no.3, pp.416-419, Jan.17.
8. F. N. Sayed, V. Grover, K. A. Dubey, V. Suarsan, A. K. Tyagi, "Solid State White Light Emitting Systems based on CeF<sub>3</sub>:RE<sup>3+</sup> nanoparticles and their composites with polymers," *Journal of Colloid and Interface Science*, vol.353, pp.445-453, Oct.25.
9. J. Boyer, F. Vetrone, L. Cuccia, J. Capobianco, "Synthesis of Colloidal Upconverting NaYF<sub>4</sub> Nanocrystals Doped with Er<sup>3+</sup>, Yb<sup>3+</sup> and Tm<sup>3+</sup>, Yb<sup>3+</sup> via Thermal Decomposition of Lanthanide Trifluoroacetate Precursors," *Journal of American Chemical Society*, vol.128, pp.7444-7445, Mar.17.
10. O. Lehmann, K. Kompe, M. Haase, "Synthesis of Eu<sup>3+</sup>-Doped Core and Core/Shell Nanoparticles and Direct Spectroscopic Identification of Dopant Sites at the Surface and in the Interior of the Particles," *Journal of American Chemical Society*, vol.126, pp.14935-14942, Dec.19.
11. S. Heer, K. Kompe, H. Gudiel, M. Haase, "Highly Efficient Multicolour Upconversion Emission in Transparent Colloids of Lanthanide-Doped NaYF<sub>4</sub> Nanocrystals," *Advanced Materials*, vol.16, no.23-24, pp.2102-2105, Dec.17.
12. H. Mai, Y. Zhang, Z. Yan, L. Sun, L. You, C. Yan, "High-Quality Sodium Rare-Earth Fluoride Nanocrystals: Controlled Synthesis and Optical Properties," *Journal of American Chemical Society*, vol.128, pp.6426-6436, Apr.20.
13. F. Wang, X. Liu, "Recent Advances in the Chemistry of Lanthanide-Doped Upconversion Nanocrystals," *Chemical Society Reviews*, vol.38, pp.976-989, Oct.13.
14. G. Qin, W. Qin, C. Wu, S. Huang, J. Zhang, S. Lu, D. Zhao, H. Liu, "Enhancement of Ultraviolet Upconversion in Yb<sup>3+</sup> and Tm<sup>3+</sup> Codoped Amorphous Fluoride Film Prepared by Pulsed Laser Deposition," *Journal of Applied Physics*, vol.93, pp.4328-4330, Apr.1.
15. G. Blaase, B. Grabmaier "Luminescent Materials," Springer, Berlin.
16. J. Boyer, J. Gagnon, A. Cuccia, J. A. Capobianco, "Synthesis, Characterization, and Spectroscopy of NaGdF<sub>4</sub>: Ce<sup>3+</sup>, Tb<sup>3+</sup>/NaYF<sub>4</sub> Core/Shell Nanoparticles," *Chemistry of Materials*, vol.19, pp.3358-3360, May.15.
17. P. Gao, Y. Xie, Z. Li, "Controlling the Size of BaF<sub>2</sub> Nanocubes from 1000 to 10 nm," *European Journal of Inorganic Chemistry*, vol.2006, no.16, pp.3261-3265.
18. H. Hu, Z. G. Chen, T. Y. Cao, Q. Zhang, M. X. Yu, F. Y. Li, T. Yi, C. H. Huang, "Hydrothermal synthesis of hexagonal lanthanide-doped LaF<sub>3</sub> nanoplates with bright upconversion luminescence," *Nanotechnology*, vol.19, pp.375702-375711, Aug.1.
19. J. L. Zhuang, J. Wang, X. F. Yang, I. D. Williams, W. Zhang, Q. Y. Zhang, Z. M. Feng, Z. M. Yang, C. L. Liang, M. M. Wu, Q. Su, "Tunable Thickness and Photoluminescence of Bipyramidal Hexagonal  $\beta$ -NaYF<sub>4</sub> Microdisks," *Chemistry of Materials*, vol.2009, no.21, pp.160-168, Oct.28.
20. F. Zhang, J. Li, J. Shan, L. Xu, D. Y. Zhao, "Shape, Size, and Phase-Controlled Rare-Earth Fluoride Nanocrystals with Optical Up-Conversion Properties," *Chemistry European Journal*, vol.2009, no.15, pp. 11010-11019.
21. J. Meng, K. Cheah, Z. Shi, J. Li, "Intense 1540nm emission from Er doped Ce:YAG phosphor," *Applied Physics Letters*, vol.91, pp.151107-151110, Oct.11.
22. J. Wang, J. Hu, D. Tang, X. Liu, Z. Zhen, "Oleic acid-modified LaF<sub>3</sub>: Er, Yb nanocrystals and their polymer hybrid materials for potential-amplification applications," *Journal of Material Chemistry*, vol.17, pp.1597-1601, Jan.15.